# PLASMA PHENOMENA AT MAGNETIC NEUTRAL POINTS

under the direction of

P.A. Sturrock



FINAL REPORT

NASA Grant NGR 05-020-512

National Aeronautics and Space Administration

Washington, D.C. 20546

February 1975


Institute for Plasma Research
Stanford University
Stanford, California

STAFF

NASA Research Grant NGR 05-020-512

PRINCIPAL INVESTIGATOR

P.A. Sturrock, Professor

FACULTY

V. Petrosian

RESEARCH ASSOCIATE

C.E. Newman

# PLASMA PHENOMENA AT MAGNETIC NEUTRAL POINTS

The object of the research carried out under this grant was to gain a better understanding of phenomena observed in experiments carried out with the plasma focus device by exploiting, if possible, the similarities between these phenomena and those exhibited by solar flares and flare-related events. It was thought that our knowledge and understanding of the solar phenomena and the mechanisms which give rise to them would provide valuable insight into the problem of explaining similar plasma focus phenomena.

With this in mind we chose to study one of the least understood aspects of the plasma focus: the origin and production of hard X-rays (energies $\gtrsim 100$ keV). The similarities between the observed plasma focus hard X-ray spectrum and the spectra of solar impulsive X-ray bursts are several, as has been previously pointed out in the literature (Elton and Lie 1972). Both require a nonthermal energy source ($kT_e \sim 1$ keV for the plasma focus); the energy spectra of both have a power law form

$$N(E) \propto E^{-\delta} \quad , \tag{1}$$

where $\delta = 3.5 \pm 1$; and the angular distribution of both spectra are observed to be anisotropic (Jalufka and Lee 1972; Petrosian 1973). In addition both spectra are presumably due to electron bremsstrahlung radiation.

The study was carried out in two phases. The first entailed finding an acceleration mechanism by which electrons could attain the hundred-kilovolt energies necessary to produce X-rays in that energy range. Current models of solar flares envision an induced electric field produced

by the motion of field lines toward the reconnection region; this $\vec{v}/c \times \vec{B}$ field accelerates particles in the vicinity of the (magnetically) neutral region toward the solar surface where they radiate and give rise to impulsive X-ray bursts by bremsstrahlung (Sturrock 1968; deJager and Kundu 1963). With this in mind we looked for an induced electric field for the plasma focus and found that, in the final stages of the collapse phase, one should expect axial electric fields, opposite in direction to the field applied by the external voltage source. This electric field is produced by the rapidly imploding current sheet, and its magnitude is given by $|\vec{v}/c \times \vec{B}_s|$, where $\vec{B}_s$ is the magnetic field just behind the current sheet. Since

$$|\vec{B}_s| = B_{s\theta} = \frac{2I}{cr_s} \quad ,$$

where $r_s$ is the distance of the current sheet from the axis and I is the current in the device, this field increases in value as the collapse phase continues. For typical values of current ($I \approx 10^6$ amp), velocity ($v \approx 2 \times 10^7$ cm/sec), and minimum radius ($r_{smin} \approx 1$ mm), the induced electric field reaches a magnitude of 400-500 kV/cm -- much larger than the externally applied field ($\approx 10$ kV/cm). In the usual mode of operation of the focus device -- center electrode positive -- the induced electric field then points toward the center electrode and, hence, accelerates electrons away from that electrode. The magnitude of this field is sufficient to produce electrons energetic enough to radiate X-rays in the hundred-kilovolt range.

The second part of our study was then to investigate the bremsstrahlung radiation to be expected from electrons accelerated by the mechanism

mentioned above. Here again we drew upon our previous work on solar X-ray bursts. Petrosian (1973) and Brown (1972) have studied the radiation produced by a beam of electrons -- with a power-law energy spectrum -- incident upon the solar surface. Their calculations account for most of the features of the solar bursts. We then undertook to perform a similar calculation for the plasma focus. Assuming the induced electric field creates a beam of electrons on the axis of the device, we first determined the shape of the energy spectrum required for the beam to produce the on-axis hard-X-ray spectrum reported by Lee et al. (1971); this spectrum was found to be a power law in energy ($N(E) \propto E^{-\alpha}$, $\alpha = 2.5 \pm 1$). We then calculated the angular distribution pattern to be expected from this beam and compared it with the observation reported by Jalufka and Lee (1972); good agreement was found. Finally, using an estimate of the total energy in hard X-rays of $10^{-2}$ joules (F. Hohl, private communication), we calculated the total number and energy of accelerated electrons required. Less than ten percent of the electrons in the plasma focus were required to be accelerated above 100 keV, but their total energy was about $10^{4}$ joules which is a significant fraction of the total energy of the device.

The work outlined above is discussed in greater detail in a paper by Newman and Petrosian (1974) which is attached as Appendix A. In conclusion, we can say that there are indeed features of solar flare processes and the plasma focus which are analogous. Our studies have shown one of these. Thus, there still remains the prospect of using laboratory experiments to study plasma processes on the sun as well as in other astrophysical systems. In order to determine whether or not this prospect is indeed a viable one, more research devoted to the study of similarities between solar and laboratory plasma phenomena will be necessary.

## REFERENCES


Brown, J. C. 1972, Solar Phys. 26, 441.

Elton, R. C. and Lie, T. N. 1972, Space Sci. Rev. 13, 747.

Jager, C. de and Kundu, M. R. 1963, Space Res. 3, 836.

Jalufka, N. W. and Lee, J. H. 1972, Phys. Fluids 13, 2858.

Lee, J. H., Loebbaka, D. S., and Roos, C. E. 1971, Plasma Phys. 13, 347.

Newman, C. E. and Petrosian, V. 1974, Stanford University Institute for Plasma Research Report No. 571 (to be published in Phys. Fluids, May 1975).

Petrosian, V. 1973, Astrophys. J. 186, 291.

Sturrock, P. A. 1968, Structure and Development of Solar Active Regions (Dordrecht:Reidel).

## APPENDIX A

"ON THE PRODUCTION OF HARD X-RAYS IN A PLASMA FOCUS"
by C.E. Newman and Vahé Petrosian, to be published
in the May 1975 issue of The Physics of Fluids.

# On the Production of Hard X-Rays in a Plasma Focus

by

C.E. Newman and Vahé Petrosian*†
Institute for Plasma Research
Stanford University
Stanford, California

## ABSTRACT

We consider a model of the plasma focus in which large axial electric fields are induced by the imploding current sheet during the final few nanoseconds of the collapse phase. This field provides a mechanism for creation of a beam of electrons of highly suprathermal energies. For such a beam, having a power-law form in energy, we calculate the bremsstrahlung radiation above 100 keV to be expected from it either from electron-deuteron collisions in the focused plasma itself or when the beam reaches the walls of the device. Upon comparison with experimental results, we conclude that the walls are the more likely source of these hard x-rays and also find qualitative agreement of the expected angular distribution of x-rays with experiment.

---

*Also Department of Applied Physics
†Alfred P. Sloan Foundation Fellow

# I. Introduction

The plasma focus device has been the subject of extensive experimental and theoretical research in recent years, and many of its features are now reasonably well understood.[1-8] A schematic of the apparatus used by NASA-Langley researchers, who have carried out the most extensive hard x-ray measurements to date, is given in Figure 1. The operation of the device can be separated into four fairly distinct phases: (1) the breakdown phase, which is initiated by closing the switch AB, causing the gas in the container to undergo dielectric breakdown and creating current flow between the two concentric electrodes; (2) the rundown phase, in which this current sheet is accelerated to the right by $\vec{J} \times \vec{B}$ forces; (3) the collapse phase, which is a continuation of the rundown phase but which begins when the current sheet reaches the end of the center electrode and undergoes rapid radial collapse, trapping, heating, and compressing some of the gas; (4) the focus phase, which is the end result of the collapse phase and in which one is left with a hot $(T_e \sim 10^7\ ^oK)$, dense $(n_e \geq 10^{19}\ cm^{-3})$ plasmoid located on the axis and having a diameter $\sim$ 1 mm and a length $\sim$ 1-2 cm. The gas used in the device is deuterium, normally at an initial pressure of 3-5 Torr, and the energy source is a 20 kv - 25 KJ capacitor bank; the center electrode is positive in normal operation.

Of the four phases, the focus phase is the most interesting as well as the least understood. The plasma is hot and dense enough for D-D fusion reactions to take place with consequent production of neutrons. This phase also entails x-ray production -- both thermal ($k \sim 1$ keV) and nonthermal hard ($k$ = 100-500 keV) x-rays. The focus phase has a lifetime of about 100 nsec. The most puzzling of the features of the focus phase are the relatively long lifetime, the anisotropy of the observed neutron

flux, and the production mechanism for the hard x-rays. It is the last of these topics which will be the subject of this paper.

Before we proceed with the description of our model for hard x-ray production, it is instructive to list the salient features of the observed hard x-ray spectrum for which any proposed model should be able to account: (1) the hard x-rays are produced in a burst about 40 nsec in length coincident (or nearly so) with the neutron production, which occurs at the time of collapse to minimum volume; (2) the spectrum of the hard x-rays in the forward (axial) direction is roughly a power law -- $\frac{dN(k)}{dk} \propto k^{-\nu}$, $k > 100$ keV and $\nu \approx 3.5 \pm 1$; (3) the angular distribution is markedly anisotropic with a broad maximum occurring between $30^{\circ}$ and $75^{\circ}$ from the forward direction; (4) estimates of the total energy radiated in hard x-rays give a value of $\sim 10^5$ ergs.[3,4,9] It is interesting to note that the observed energy spectrum in the plasma focus is similar to that observed in solar x-ray bursts associated with solar flares which has been noted elsewhere.[10] Thus it is possible that an understanding of the x-ray-producing processes in the plasma focus may lead to a better understanding of those in solar flares.

There are three candidates for the source of the observed hard x-rays -- the face of the center electrode, the focused plasma itself, and the walls of the aluminum vacuum vessel. In his paper on the simulation of the plasma focus, Potter[7] proposes that the collapsing current sheet gives rise to an induced $\vec{v} \times \vec{B}$ electric field of strength $\sim 10^5$ v/cm on the axis; this field strength is far above that needed for electron runaway so a substantial number of electrons are accelerated to high energies toward the anode; the hard x-rays are then a result of anode bombardment by these

electrons. There are two objections to this proposed mechanism. First, the anode can be eliminated as a source by using a hollow center electrode; when this is done, the hard x-rays are still observed, and the spectrum differs very little from the solid center electrode case. Second, as we will see in the next section, the direction of this induced electric field is toward the center electrode, hence electrons are accelerated away from the anode. Thus we are left with the other two as possible sources for the hard x-rays; we treat both cases in this paper.

Our model, then, is the following: the fast radial collapse of the current sheet produces an induced axial electric field which accelerates electrons away from the anode; in the final stages of collapse, this field rises to a sufficiently high value in the trapped plasma to accelerate thermal electrons to a few hundred keV; these electrons then radiate by bremsstrahlung either in collisions with ions in the plasma itself or upon colliding with the walls of the container. The model is described in detail in Section II; in Section III we treat the two cases -- radiation in the focus and radiation in the walls -- and explore the consequences of each; in Section IV we present our conclusions and suggest an experiment to ascertain the actual hard x-ray source.

## II. Theoretical Model

We assume that the current in the sheet is constant throughout the collapse phase; this is consistent with experimental observations which show the current to have a roughly constant value $\sim$ 500 KA until the focus stage is reached, at which time the current drops rapidly.[1,2,4] We also assume for simplicity that the current sheet is infinitely thin; this

latter assumption is not crucial since our results would be changed very little were we to assume small but finite sheet thickness. Neglecting displacement current the magnetic field at any point is given from Ampere's law,

$$\nabla \times \vec{B} = \frac{4\pi}{c} \vec{J} \quad . \tag{1}$$

We assume $\vec{J}$ is in the rz-plane (from symmetry) so that $\vec{B}$ is toroidal and given by

$$B_\theta(r,z) = \frac{2I}{cr} \Theta[t-t_0(r,z)] \quad , \tag{2}$$

where $I$ is the total current, $\Theta$ is a Heaviside function of its argument and $t_0(r,z)$ is the time at which the moving current sheet passes through the point $(r,z)$. Thus the magnetic field at a given point vanishes until the current sheet reaches that point, at which time it jumps to the value $B_\theta = \frac{2I}{cr}$ and remains at that constant value throughout the remainder of the collapse phase.

The electric field may then be found from Faraday's law

$$\nabla \times \vec{E} = -\frac{1}{c} \frac{\partial \vec{B}}{\partial t} = -\frac{1}{c} B_\theta \delta[t-t_0(r,z)] \hat{\theta} \quad . \tag{3}$$

From (3) we see that the component of $\vec{E}$ tangential to the sheet also has a discontinuity at the sheet. Referring to Figure 2, we see that as we pass from region A behind the sheet to region B ahead of the sheet, the jump condition satisfies the following condition

$$\left(\vec{E}^B - \vec{E}^A\right) \cdot \frac{\vec{J}}{|\vec{J}|} = \left(\frac{\vec{J}}{|J|} \times \frac{\vec{v}}{c}\right) \cdot \vec{B}_\theta = \left(\frac{\vec{v}}{c} \times \vec{B}_\theta\right) \cdot \frac{\vec{J}}{|\vec{J}|}$$

or

$$\vec{E}^B - \vec{E}^A = \frac{\vec{v}}{c} \times \vec{B} \quad , \tag{4}$$

where $\vec{v}$ is the velocity of the current sheet. Now from (3) we see that $\nabla \times \vec{E} = 0$ in both regions A and B separately so that $\vec{E}$ is derivable from a potential in each region; however, we know that

$$\int_{CE}^{OE} \vec{E}_A \cdot d\vec{\ell} = V_0 \tag{5}$$

where $V_0$ is the applied voltage and CE and OE denote the center and outer electrodes. This equation holds for any path lying entirely within region A.

Let us now consider the final stages of collapse and examine the focus region. We take as parameters

$$r \sim 1 \text{ mm} \quad ,$$
$$v \sim 2 \times 10^7 \text{ cm/sec} \quad ,$$
$$I \sim 500 \text{ KA} \quad ,$$

all of which are typical values obtained in the laboratory. Since, near the focus, the current sheet is nearly along the z-axis, we can take $\vec{v}$ to have an inward radial component only, and we find

$$E_z^B - E_z^A = \frac{2}{3} \times 10^3 \text{ esu} = -200 \text{ kV/cm} \quad . \tag{6}$$

Since (5) must be satisfied by $E^A$, with $V_0 \approx 20$ kV and the path length for the integral $\sim$ few cm, we conclude that $|E_z^B| \gg |E_z^A|$ and thus $E_z^B \approx -200$ kV/cm. This axial electric field is thus strong enough to

accelerate electrons to a few hundred kilovolts as long as $r$ is small enough, i.e., during the last stages of collapse. (Note that if $r = 2$ mm, $E_z^B \approx -100$ kV/cm, which is still a high enough value to give significant acceleration; the sheet travels from $r = 2$ mm to $r = 1$ mm in 5 nsec which is sufficient time to accelerate electrons to a relativistic velocity with these field strengths.) However, these electrons are accelerated away from the center electrode, not toward it, as Potter proposed;[7] ions presumably will be accelerated toward the anode during this stage of focus development. Evidence for axial particle acceleration away from the anode has been reported by Lee,[11] who noted that after a number of runs, a spot was formed on the vacuum vessel wall where it intersects the axis (the point designated by C in Figure 1).

That the axial field is opposite in sign from the field due to the source voltage has also been pointed out in a paper by Gary and Hohl,[6] who made extensive revisions to Bernstein's model for ion acceleration.[5] Bernstein found a jump condition analogous to that given by (4), but he assumed $E_z = 0$ at $r = 0$ as a boundary condition. As is evident from the arguments given here, we feel that such an assumption is unjustified.

We should also mention that this electric field is opposite in sign to that which accelerates ions in the model of Gary and Hohl[9] since ions in that model are also accelerated away from the anode. This apparent contradiction is resolved if we note that the accelerating field of Gary and Hohl is due to $\dot{I}$, not the motion of the current sheet. The field due to $\dot{I}$ is somewhat smaller in magnitude ($\sim$ few kV/cm) than the field computed above, hence it does not become important until the motion of the sheet ceases. Thus the acceleration of electrons and production of x-rays

occurs during the last few nanoseconds of the collapse phase while the ion acceleration and neutron production takes place at the beginning of the focus phase. This extremely short time interval between these two events then accounts for the apparent coincidence of the neutron and hard x-ray pulses.[4]

Given now that we have a strong axial field capable of accelerating electrons to mildly relativistic energies, we now turn to the treatment of their subsequent bremsstrahlung radiation.

## III. Bremsstrahlung Radiation

In this section we calculate the expected hard x-ray production by the accelerated electrons via bremsstrahlung. Most of the aspects of this problem have been studied by various authors in connection with the impulsive solar x-ray bursts. We shall make frequent use of the results in the paper by Petrosian.[12*] Briefly, the electrons lose energy via elastic collision and bremsstrahlung as [cf. equations I.1 and I.13)

$$\dot{E}_{coll} = -2\pi r_0^2 \, nZc \, \ell n\Lambda/\beta \quad , \qquad d\dot{E}_{brem} = -d\sigma_{brem} \, nc\beta k \tag{7}$$

where $r_0$ is the classical electron radius, $n$ and $Z$ are the density and charge of the target particles, $\beta$ is the velocity of the electrons (in units of $c$ the speed of light), $k$ is the energy of the bremsstrahlung x-ray (all energies will be expressed in units of electron rest mass energy $mc^2$), $\Lambda$ is given in equations I.2 and I.3, and $d\sigma_{brem}$ is the bremsstrahlung cross section. In what follows we shall use the non-relativistic approximation

---

*We shall denote the equations and figures from this paper by a prefix I.

$$d\sigma_{brem} = \frac{16}{3}\,\alpha r_0^2\, Z^2\, \frac{1}{k}\left\{\frac{dk}{2E}\,\ell n\,\frac{1+\sqrt{1-k/E}}{1-\sqrt{1-k/E}}\right\} \quad , \tag{8}$$

where $E$ is the electron kinetic energy and $\alpha = 1/137$, and the approximation [cf. equation I.29 and I.30]

$$\int_k^E k'\,d\sigma'_{brem} = \frac{16}{3}\,\alpha r_0^2\, Z^2 (1-k/E)^2 \quad . \tag{9}$$

Since the spectrum of the observed hard x-rays can be approximated by a power law we assume a truncated power law electron spectrum:

$$dN(E) = N\,\delta\left(\frac{E}{E_1}\right)^{-\delta-1} dE/E_1 \quad \text{for} \quad E > E_1 \quad , \tag{10}$$

and $dN(E) = 0$ for $E < E_1$, so that $N$ is the total number of the accelerated electrons and

$$\mathcal{E}_e = \frac{\delta}{\delta-1}\,NE_1 \tag{11}$$

is the total energy of these electrons. We use these expressions to derive first the required values of $\mathcal{E}_e$, $N$ and $\delta$ assuming that the x-rays are produced in the focus and/or in the aluminum walls. The expected angular distributions are discussed at the end of this section.

a. X-Ray Production in the Focus

In the focus, ($n \leq 10^{20}$, $Z = 1$, $\ell n\Lambda = 30$) the "mean free path" for 100 keV electrons ($E = 1/5$, $\beta = 0.6$) defined as $\lambda \equiv -c\beta\, E/\dot{E} \approx E\beta^2/[2\pi r_0^2 nZ\ell n\Lambda]$ $\approx 50$ cm, so that the electrons will escape the focus region with little loss of energy, and the thin target calculation applies here. Let $J(k)$

be the differential spectrum of the emitted x-rays and $\mathcal{E}(k) = \int_k^\infty J(K')dk'$ be the integral energy spectrum (observations show that for $k > 100$ keV, $\mathcal{E}(k) \propto k^{-\nu+2}$, $\nu = 3.5 \pm 1$, and $\mathcal{E}(100\ \text{keV}) \approx 10^{-2}$ joules). We find it simpler to express our results in terms of the latter quantity.

It is easy to show that equations (7) to (10) give

$$\mathcal{E}(k) = -\int_{E_1}^{\infty} dN(E) \int_k^E dk' \int_\ell \frac{d\dot{E}_{brem}}{dk'} \frac{d\ell}{c\beta} = \frac{16}{3} \alpha r_0^2 N \int n d\ell \begin{cases} \left(\frac{k}{E_1}\right)^{-\delta} \frac{2}{(\delta+1)(\delta+2)} & , \quad k > E_1 \\ 1 - \frac{2\delta}{\delta+1}\frac{1}{E_1} + \frac{\delta}{\delta+2}\left(\frac{k}{E_2}\right)^2 & , \quad k < E_1 \end{cases} . \tag{12}$$

Here $\mathcal{E}(k)$ is expressed in units of $mc^2$ and $d\ell$ is the differential path length in the focus. For $k > E_1$ this spectrum is a power law with index $-\delta$ and flattens out rapidly for $k < E_1$. Assuming $E_1 \approx 100$ keV and $\int n d\ell \approx 2 \times 10^{20}$ cm$^{-2}$, we find for $\mathcal{E}(100\ \text{keV})$ and the bremsstrahlung yield

$$\mathcal{E}(100\ \text{keV}) \approx \frac{4 \times 10^{-20}}{(\delta+1)(\delta+2)} N \text{ joules} \quad , \quad Y(E_1) = \frac{\mathcal{E}(E_1)}{\mathcal{E}_e} = \frac{2.5 \times 10^{-6}(\delta-1)}{\delta(\delta+1)(\delta+2)} \times \frac{100\ \text{keV}}{E_1} . \tag{13}$$

Comparing these with observation we obtain

$$\delta \approx 1.5 \pm 1 \quad , \quad N \approx (4 \text{ to } 1) \times 10^{18} \text{ particles} . \tag{14}$$

This is a stringent requirement, since it implies that more than ten percent of the total electrons in the focus [$\approx \pi r^2 \int n d\ell \approx 6 \times 10^{18} (n/10^{20}\text{cm}^{-3})$] must be accelerated to energies greater than 100 keV, with a total energy of $\mathcal{E}_e \approx 4 \times 10^4$ joules, which is greater than the total energy input of

the device. For $E_1 \approx 200$ keV, N is reduced by a factor of 2 but $\mathcal{E}_e$ remains the same. Furthermore, as shown below, these electrons will emit much more hard x-rays when interacting with the walls of the device, unless they are decelerated to lower energies before reaching the walls. Note that the quantity $\int n d\ell$ for the gas outside the focus is about $10^{18}$ cm$^{-2}$ so that x-ray emission between the focus and the walls is negligible.

B. X-Ray Production in the Walls

In the aluminum walls (thickness $\sim 0.2$ cm), $n \approx 6 \times 10^{22}$, $Z = 13$, $\ell n\Lambda = 14$ [cf. Evans[13]] the "mean free path" of 100 keV electrons is less than 0.02 cm, so that the thick target calculations apply here. In this case it can be shown that the spectrum is [cf. equations I.20 and I.28]

$$\mathcal{E}(k) = \frac{16}{3}\frac{\alpha Z N}{2\pi \ell n\Lambda} E_1^2 \begin{cases} (k/E_1)^{-\delta+2}\,\dfrac{4}{(\delta-2)(\delta-1)\delta} & , \quad k > E_1 , \\ \left[\dfrac{\delta}{\delta-2} - 4\dfrac{k}{E_1}\dfrac{\delta}{\delta-1} + \left(\dfrac{k}{E_1}\right)^2\left(\dfrac{2+3\delta}{\delta} - 2\ell n\dfrac{k}{E_1}\right)\right] & , \quad k < E_1 . \end{cases} \tag{15}$$

This spectrum is also a power law with index $-\delta+2$ for $k > E_1$ and flattens out rapidly for $k < E_1$. For $E_1 \approx 100$ keV we obtain

$$\mathcal{E}(100\text{ keV}) = \frac{2.9 \times 10^{-17}}{\delta(\delta-1)(\delta-2)} N \text{ joules} \quad \text{and} \quad Y(100\text{ keV}) = \frac{4.6 \times 10^{-3}}{(\delta-2)\delta^2} . \tag{16}$$

Comparing these with observations we find

$$\delta = 3.5 \pm 1 , \quad N = (1.3 \text{ to } 0.6) \times 10^{16} , \quad \mathcal{E}_e = 10^{-2}/Y(100\text{ keV}) = (10 \text{ to } 100)\text{ joules} . \tag{17}$$

For $E_1 = 200$ keV the required number of electrons and their energy will be reduced by an order of magnitude.

As is evident from equations (14) and (17) it is more efficient to produce the x-rays in the walls. Most of the energy in this case is deposited in the wall. If the electrons remain on the axis, an energy of about 20 joules will be deposited on a spot on the axis of the device. After 500 discharges, this energy amounts to about $10^4$ joules which could create a hole of about one centimeter in diameter in the 2 mm thick aluminum wall as observed by Lee.[11]

c. Angular Distribution of the X-Rays

So far we have treated the problem in the non-relativistic approximation where the angular distribution of bremsstrahlung radiation from a beam of electrons peaks in directions perpendicular to beam axis. However, for relativistic energies, the radiation is concentrated in the forward direction along the axis. For semi-relativistic particles ($E \sim 100$ keV) the radiation peaks in a direction between the forward direction and directions perpendicular to the beam; for example, 100 keV x-rays emitted by electrons with 150 keV peak in a direction about 40 degrees from the axis [cf. Figure I.2a]. For a power law electron spectrum of $\delta \geq 5$, the 100 keV photons will have a flat distribution between 0 to $60^\circ$ from the axis then begin to decrease rapidly at wider angles [cf. dashed lines in Figure I.4]. This effect is independent whether the target is thin or thick. However, for a thick target the collisions will disperse the beam and cause a wider angular distribution.[14] This agrees approximately with the observed distribution. We do not attempt a more rigorous comparison of our model with the experimental results because these results are still

tentative, having been obtained only once and with large experimental uncertainties.

## IV. Summary and Conclusions

We have shown that large axial electric fields, capable of accelerating electrons to mildly relativistic energies, can be induced by the rapid radial collapse of the current sheet in the plasma focus. The observed anisotropic angular distribution and the energy spectrum of the hard x-rays from the plasma focus appear to show that the mechanism for the production of these x-rays might be bremsstrahlung from a directed beam of such electrons. If the radiation is produced in the focus, then a very efficient acceleration mechanism is required whereby a considerable fraction of electrons in the focus are accelerated carrying most of the energy input of the device. This appears to be unlikely. In addition, these electrons must be stopped or slowed down to lower energies before reaching the walls of the device. Otherwise, they will produce one hundred to a thousand times more x-rays at the walls. Even if these electrons are slowed down to lower energies, say to few keV's, each discharge will deposit more than $10^3$ joules of energy in the walls which must have obvious observable consequences after each discharge if the beam is not dispersed, or after repeated discharges, even if the beam is completely dispersed before reaching the walls. For this reason, we consider bremsstrahlung in the focus as an unlikely mechanism for the hard x-ray production.

On the other hand, if the x-rays are produced in the wall along the axis of the device, only a small fraction (less than 0.1%) of the electrons need to be accelerated carrying a few joules of energy. The observed damage on the wall appears to favor this hypothesis. However, in the

experiment for the determination of the angular distribution of the x-rays, the detectors were focused on the focus region rather than the spot on the wall. If the angular resolution of the detector was sufficiently fine to distinguish between these two sources, then x-ray emission from the spot on the wall must also be ruled out.

It would be desirable to repeat the angular distribution experiment with higher spectral and spatial resolution for further testing of this model. In particular, an additional detector focused on the spot on the wall at right angles to the axis could distinguish easily between these two sources. Another test of the bremsstrahlung radiation would be determination of the polarization characteristics of these x-rays. In directions perpendicular to the beam axis, the percentage of radiation polarized perpendicular to the plane of the electron beam and line of sight could be as high as 90 percent for production in the focus and lower (60 percent) for production in the wall because of scattering.[14] Polarization up to 60 percent has been observed in the solar impulsive x-ray bursts.[15]

## Acknowledgments

We would like to thank S. Peter Gary and Peter A. Sturrock for many helpful discussions. This work was supported by the National Aeronautics and Space Administration under Grants NGL 05-020-272 and NGR 05-020-512.

## References


1. J.W. Mather, Methods of Experimental Physics (Academic Press, New York, 1971), Vol. 9B, pp. 187.

2. J.W. Mather and P.J. Bottoms, Phys. Fluids 11, 611 (1968).

3. J.H. Lee, D.S. Loebbaka, and C.E. Roos, Plasma Phys. 13, 347 (1971).

4. N.W. Jalufka and J.H. Lee, Phys. Fluids 15, 1954 (1972).

5. M.J. Bernstein, Phys. Fluids 13, 2858 (1970).

6. S.P. Gary and F. Hohl, Phys. Fluids 16, 997 (1973).

7. D.E. Potter, Phys. Fluids 14, 1911 (1971).

8. D.E. Potter and M.G. Haines, Plasma Physics and Controlled Nuclear Fusion Research (International Atomic Energy Agency, Vienna, 1971), Vol. I, pp. 611.

9. F. Hohl (private communication to P.A. Sturrock).

10. R.C. Elton and T.N. Lie, Sp. Sci. Rev. 13, 747 (1972).

11. J.H. Lee (private communication to C.E. Newman).

12. V. Petrosian, Astrophys. J. ~~185, 359~~ 186, 291 (1973).

13. R.D. Evans, The Atomic Nucleus (McGraw-Hill, New York, 1955), p. 582.

14. J.C. Brown, Sol. Phys. 26, 441 (1972).

15. I.P. Tindo, V.D. Ivanov, S.L. Mandelstam, and A.I. Shuryghin, Sol. Phys. 24, 429 (1972).

## Figure Captions

Figure 1. Schematic diagram of experimental apparatus on which hard measurements were carried out. Also depicted are the processes leading to the formation of the plasma focus and the direction of the induced electric field, which is described in Section II. The walls of the vacuum vessel are made of 2mm-thick aluminum and the point C denotes the point at which a spot was formed - evidently due to bombardment by energetic particles and leading to leaks in the vacuum system after a few hundred runs.[11]

Figure 2. Reference diagram for computing the jump condition for the electric field across the current sheet during collapse.

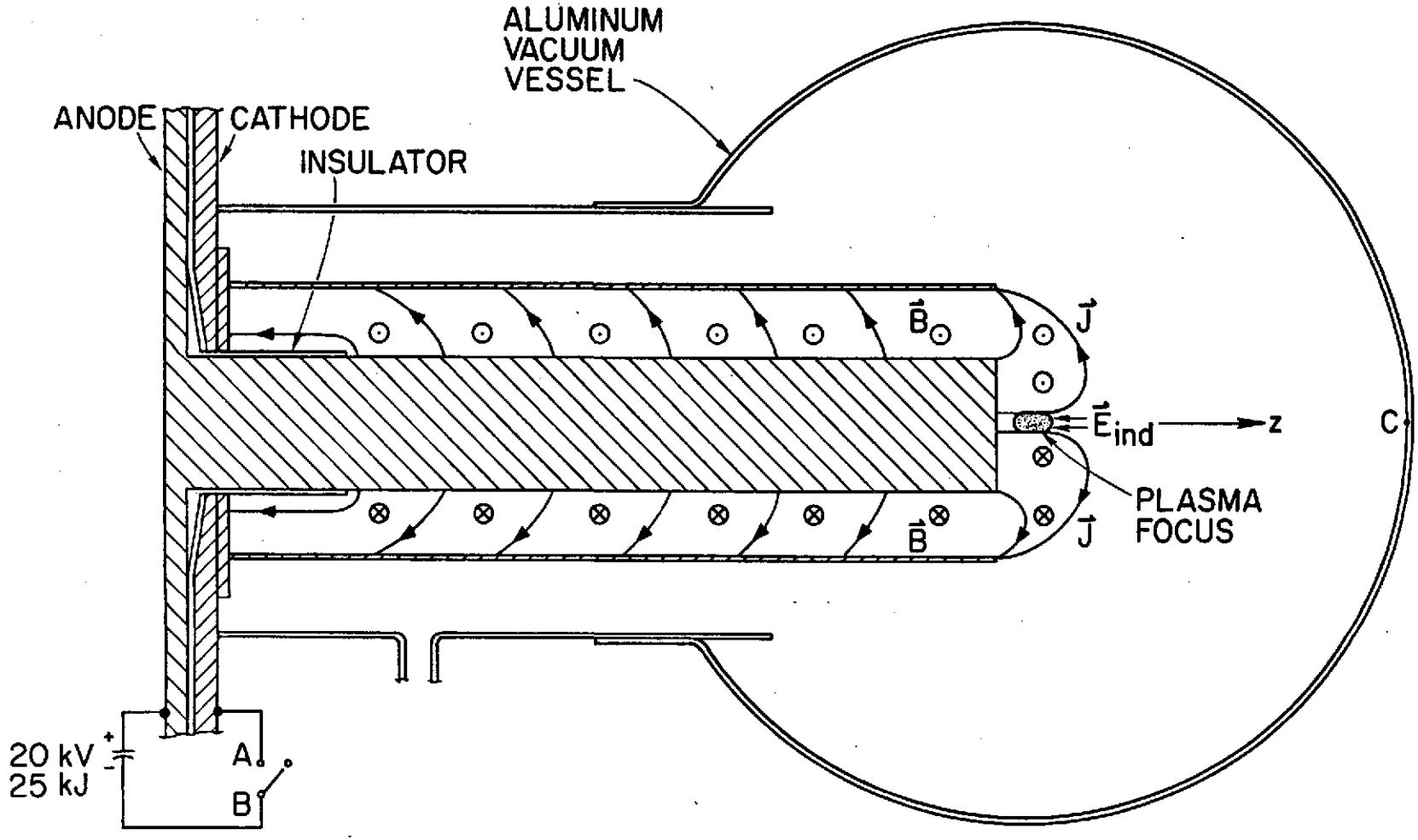
ALUMINUM
VACUUM
VESSEL
ANODE
CATHODE
INSULATOR
$\vec{B}$
$\vec{J}$
$\vec{E}_{ind}$
z
C
PLASMA
FOCUS
$\vec{B}$
$\vec{J}$
20 kV
25 kJ
+
-
A
B

Figure 1

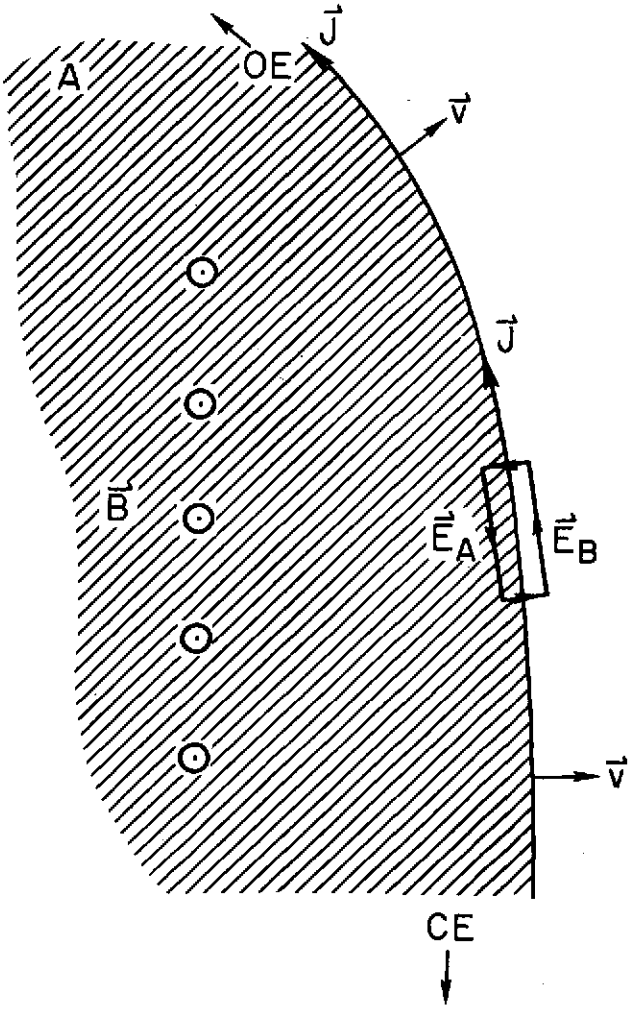


Figure 2